

Fabrication of Hexagonal CuCoO₂ Modified Screen-Printed Carbon Electrode for the Selective Electrochemical Detection of Furaltadone

Kiruthika Mariappan, Tse-Wei Chen^{1,2}, Shen-Ming Chen^{*}, Tien-Wen Tseng^{1,*}, Yongzhong Bian^{3,4}, Ting-Ting Sun^{3,*}, Jianzhuang Jiang^{3,4,*}, Jaysan Yu⁵

¹ Department of Chemical Engineering and Biotechnology, National Taipei University of Technology, No. 1, Section 3, Chung-Hsiao East Road, Taipei 106, Taiwan, ROC.

² Research and Development Center for Smart Textile Technology, National Taipei University of Technology, Taipei 106, Taiwan, ROC.

³ Beijing Key Laboratory for Science and Application of Functional Molecular and Crystalline Materials, Department of Chemistry, School of Chemistry and Biological Engineering, University of Science and Technology Beijing, Beijing 100083, China

⁴ Daxing Research Institute and Beijing Advanced Innovation Center for Materials Genome Engineering, University of Science and Technology Beijing, Beijing 100083, China

⁵ Well Fore special wire corporation, 10, Tzu-Chiang 7rd., Chung-Li Industrial Park, Taoyuan, Taiwan

*E-mail: smchen78@ms15.hinet.net (S.M.C.), f10403@ntut.edu.tw (T.W.T.), ttsun99@ustb.edu.cn (Y.B.), Jianzhuang@ustb.edu.cn (T.T.S.)

Received: 12 March 2022 / Accepted: 2 April 2022 / Published: 7 May 2022

Furaltadone (FTD) is one of the veterinary drugs from the class of nitrofurans. Mostly the toxicity of the organic elements is very harmful, hence the toxic nature of FTD affects human health and the biosphere by inappropriate exuding of organic toxic elements. The as-prepared inorganic complex was characterized by field emission scanning electron microscope (FESEM), and X-ray diffraction (XRD) studies. Hydrothermally prepared copper-cobalt oxide (CuCoO₂) is adorned on an activated screen-printed carbon electrode (ASPCE) for the detection of FTD by electrochemical methods which are Cyclic Voltammetry (CV), and Differential Pulse Voltammetry (DPV). The fabricated ASPCE/CuCoO₂ electrode exhibits outstanding limits of detection (1.79 nM), high sensitivity (21.03 $\mu\text{A } \mu\text{M}^{-1} \text{cm}^{-1}$), and broad linear range (0.1-316 μM). The study of interference represents that metal ions and the nitro group have no impact on the FTD determination. Consequently, the ASPCE/CuCoO₂ electrode reveals creditable for repeatability, reproducibility, and stability. Notably, this sensing platform also exhibits excellent performance in determining the FTD contents in Antibiotic samples, which suggests great potential for real-time applications.

Keywords: Copper cobalt dioxide; Furaltadone; Electrochemical sensor; Screen-printed carbon electrode; Low detection limit.

1. INTRODUCTION

Furaltadone (FTD) is the class of nitrofurans that is antiprotozoal antiseptic material [1, 2]. It has broad-spectrum antimicrobials, which has characteristics of the 5-nitrofurans ring, which is capable of feeding supplement on widening advancements and used for the treatment of protozoan and bacterial infections [3]. The contamination of FTD in food is transformed into chemical species which are, 3-amino-5-morpholino ethyl-2-oxazolidone, semicarbazide (SEM), or 1-aminohydantoin (AHD). The metabolism of such compounds is very harmful to human health [4]. FLD is produced and used legally in several nations due to its efficacy and inexpensive cost. Therefore, the need to detect the amount of FTD in the food of market is important, due to the reason carcinogenicity in their remnant in food or water causes diseases for human health [5]. FLD residues are now identified using high-performance liquid chromatography (HPLC), liquid chromatography-tandem mass spectrometry (LC-MS), and enzyme-linked immunosorbent assays (ELISA). On the other hand, traditional approaches are expensive, time-consuming, and require large instrumental equipment to finish the analysis. As a result, a low-cost, rapid, and easy implementation technique is more important and required [6,7].

Electrochemical methods are more beneficial, inexpensive, highly sensitive, simple, rapid analyzing, flexible, and applicable for analyzing various samples in the pharmaceutical, and environmental fields [8,9]. Nowadays, the electrochemical sensor has concurrent analysis of species, electrode compactness, and advanced materials operations [10,11]. Hence, a screen-printed electrode (SPCE) is an excellent working electrode to construct thick-film transducers, this method is highly repeatable and easy to prepare. The SPCE is disposable, affordable, and easily portable. Besides, this electrode is reported as a way of modifying the surface by metal complexes, which leads to improving electrochemical reactivity, and specific sensitivity of the electrode [12,13]. This electrode works with other electrodes such as reference electrodes and counter electrodes constructed on substrates like conductive metals such as nanoparticles, nanocomposites, and metal complexes [14-16]. The metal complex adorned SPCE involved in real samples, and adequate results were observed [17,18]. This method is improved to work with very low volume samples. The scope of applications incorporates environmental analysis, clinical, and food [19].

As a result, for successful detection of FTD at low overpotential, metal complex modification of the SPCE surface is required. Metal complexes are the best options for oxidizing FTD at lower overpotential. Delafossite oxides particular is important in electrochemical sensors with high electrocatalytic activity, electron transfer properties, and high sensitivity [20,21]. CuMO_2 ($M = \text{Al, Ga, Cr, Co, etc.}$) based on delafossite oxides are an essential class of transition metal oxides. CuMO_2 oxides have been widely testified to be used in the fields of translucent conductive oxides, solar cell devices, photocatalysis, and other optoelectronic devices as p-type semi-conductive materials [22]. Besides, CuMO_2 oxides such as CuCrO_2 , CuGaO_2 , and CuCoO_2 have all been shown to be effective electrocatalysts in the water splitting to oxygen evolution pathway. Moreover, copper-cobalt dioxide (CuCoO_2) has strong electrocatalytic activity as well as long-term stability in electrocatalysis. Further, CuCoO_2 had a 3D orbital of copper and 2p orbital hybridization of oxygen, as well as a primary conductive hexagonal copper layer. The CuCoO_2 is highly conductive and has promising applications in electronics and optoelectronic devices [22-23]. The CuCoO_2 shows a large electrochemical surface area,

improved conductivity, fast electron transfer, and ion transport rate, shows very good electrochemical properties, very good cyclic stability, and higher rate capacity. In CuCoO_2 , copper cation stimulates excellent electric conductivity and can transport the electron has relatively very low activation energy uniting the metal species. CuCoO_2 plays important role in various fields such as electrocatalytic activities and supercapacitors [24]. Further, the shape of CuCoO_2 is important for increasing specific surface area and electrocatalytic activity. The CuCoO_2 crystal has a hexagonal arrangement with alternating layers of linearly coordinated O–Cu–O and edge-sharing octahedral CoO_6 . The hexagonal structure of CuCoO_2 has received a lot of interest because of its strong electrocatalytic activity, and good thermoelectric performance. The hexagonal structure of CuCoO_2 is considered an electrode material as a result of its strong electrocatalytic activity and long-term stability toward electrochemical sensors [25-27]. Here, the CuCoO_2 complex modified on SPCE was used for the electrochemical determination of FTD. The SPCE/ CuCoO_2 method was used to detection of FTD in this investigation. The electrochemical methods used here are straightforward, quick, and non-toxic, and it doesn't necessitate high temperatures or lengthy protocols. The ASPCE/ CuCoO_2 electrode was good, with considerably improved electrocatalytic properties such as a low detection limit and a broad linear range towards the detection of FTD [28]. Hence, the prepared CuCoO_2 nanoparticles were a facile preparation method, cost-efficient, and show excellent applications in electrocatalysis, supercapacitors, and electrochemical sensors. In this study, the hexagonal structure of CuCoO_2 was produced by the hydrothermal method and used for the sensitive and selective determination of FLD. In this work, the CuCoO_2 complexes non-covalently interacted on the ASPCE surface. Besides, the ASPCE/ CuCoO_2 electrode has been exhibited a very low-level detection limit and higher electrode sensitivity due to the enhanced electrochemical activity and broad surface area.

2. EXPERIMENTAL

2.1. Materials and Methods

Screen-printed carbon electrodes (active surface area = 0.08 cm^2) were purchased from Zensor R&D Co., Ltd., Taipei, Taiwan. Copper (II) nitrate trihydrate ($\text{Cu}(\text{NO}_3)_2 \cdot 3\text{H}_2\text{O}$, 99%), Cobalt (II) nitrate hexahydrate ($\text{Co}(\text{NO}_3)_2 \cdot 6\text{H}_2\text{O}$, 99.0%), Furaladone hydrochloride and sodium hydroxide were purchased from Sigma Aldrich chemical company Taiwan. Na_2HPO_4 (0.05 M) and NaH_2PO_4 (0.05 M) were used to make phosphate-buffered saline (PBS; pH = 7). Further, H_2SO_4 (0.5 M) and NaOH (2 M) were used to alter the pH conditions. The crystalline structure of CuCoO_2 was determined using the X-ray diffraction (XRD, PANalytical X'PERT PRO, Netherlands) using Cu-K α as source radiation ($\lambda = 1.5417 \text{ \AA}$), Field emission scanning electron microscope (FESEM JEOLJSM-6500F) was used to characterize the surface morphology of the nanoparticles. A HORIBA EMAX X-ACT was used to do the elemental analysis (model 51-ADD0009). The electrochemical studies were examined by a regular three-electrode system which is an SPCE as a working electrode (area= 0.035 cm^2), platinum (Pt) wire acted as a counter electrode, and Ag/AgCl (saturated KCl) was used for the reference electrode. Differential Pulse Voltammetry (DPV), Cyclic voltammetry (CV), Amperometric (i-t) studies were studied by the CHI 120 electrochemical work station at Ambient temperature. Tetracycline and Silver

zine antibiotic ointment were purchased from a local pharmacy in Taipei, Taiwan. The electrolyte in the electrochemical cell was deoxygenated for 15 minutes with pure N_2 . All the experiments were carried out at room temperature, with double distilled water used to make all of the reaction solutions.

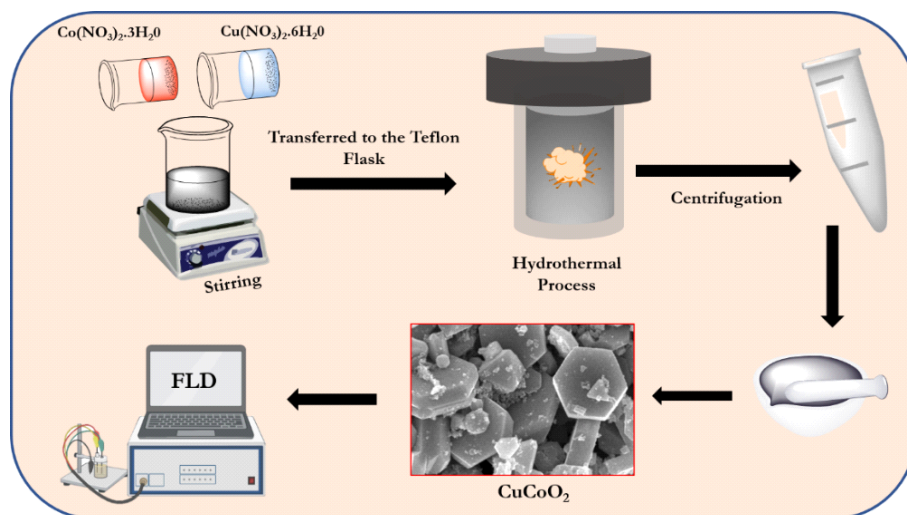
2.2 Synthesis of hexagonal structure of $CuCoO_2$

The hexagonal structure of $CuCoO_2$ was synthesized by the hydrothermal process. Copper (II) nitrate trihydrate (20g), Cobalt (II) nitrate hexahydrate (20g) is dissolved in 14 mL of distilled water, after continuous stirring sodium hydroxide was added and further continued for 20 minutes. Then, the solution was transported to a Teflon-coated autoclave and utilized for the hydrothermal reaction at $100^\circ C$ for 24 hrs, after cooling down the reaction the temperature was reduced gradually then washed the $CuCoO_2$ nanoparticles with distilled water and ethanol many times. Further kept in the process of calcination under the temperature of $400^\circ C$ for 2hrs [29].

2.3 Preparation of ASPCE/ $CuCoO_2$

The ASPCE was prepared by following previously reported procedures [30, 31]. In detail, the bare SPCE was cleaned utilizing a sonication bath with ethanol-containing water to eliminate the adsorbed pollutants on the SPCE surface. The washed SPCE was then placed in an electrochemical cell containing PBS (pH 7) and KCl, and a potential difference of 0-2.0 V was applied for 10 cycles to activate the SPCE and formed ASPCE. After the procedure of activation, the ASPCE electrode was desiccated at room temperature for further usage.

The synthesized $CuCoO_2$ dispersed in absolute ethanol and it was sonicated for 2 to 3 hours to get a homogenous solution. After the sonication, the $CuCoO_2$ was gently coated with Activated SPCE (ASPCE) about $10 \mu L$ and it was permitted to dry in the oven. Then the ASPCE/ $CuCoO_2$ was constructed and submerged in the solution of 0.1M PBS by applying the potential the FTD was detected [32,33]. For further studies, the ASPCE/ $CuCoO_2$ was permitted to construct by the same procedure (Scheme 1) [34,35].



Scheme 1. Preparation of hexagonal $CuCoO_2$ and it used for the FTD electrochemical sensor.

3. RESULT AND DISCUSSION

3.1 Characterization of hexagonal structure of CuCoO_2

The nanostructure, morphology, and chemical conformation of the CuCoO_2 complex were studied by FESEM with EDX. The crystalline arrangements were examined by XRD studies. Figure. 1A & B represents the FESEM image of CuCoO_2 shows the delafossite hexagonal structure with the size of these hexagonal is around 200 to 300 nm. Figure. 1 shows the XRD spectra of CuCoO_2 complex (JCPDS card No. 21-0256) expressed at the diffraction peak at 28.5° , 31.5° , 36.9° , 37.7° , 58.5° , and no impurities were present. The XRD studies represent that the CuCoO_2 was obtained at the hydrothermal synthesis at a low-temperature 100°C for 24 hr.

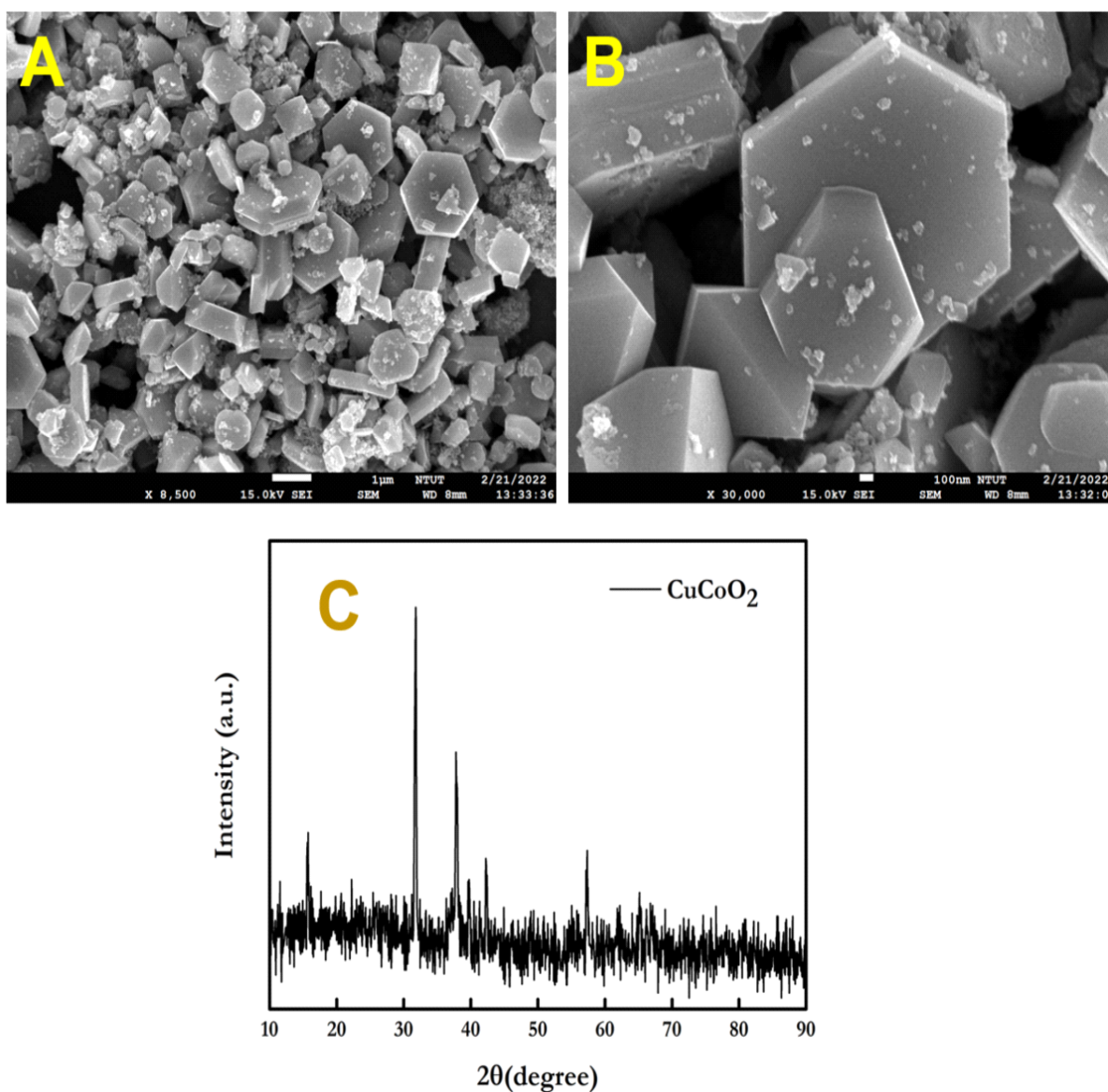


Figure 1. FESEM images CuCoO_2 (A & B), and (C) XRD patterns of CuCoO_2 .

Figure. 2A shows the elemental mapping analysis revealed a uniform distribution of Copper (Cu), Cobalt (Co), and Oxygen (O) has observed in the picked region of the CuCoO_2 complex. **Figure. 2B-D** shows the elemental mapping analysis established that Cu, Co, and O were evenly distributed throughout the CuCoO_2 complex. **Figure. 2E** shows the Energy-dispersive X-ray spectroscopy (EDS) of CuCoO_2 analyzed in the scanning transmission electron microscopy shows the EDX spectrum of CuCoO_2 has revealed that the complex comprised of Copper (Cu), Cobalt (Co), and Oxygen (O). **Figure. 2F** exhibits the quantitative analysis of the CuCoO_2 complex showing the weight of Copper at 44.4%, Cobalt at 39.8%, and Oxygen at 15.9%. Hence, the EDX spectra confirm the good formation of the CuCoO_2 complex.

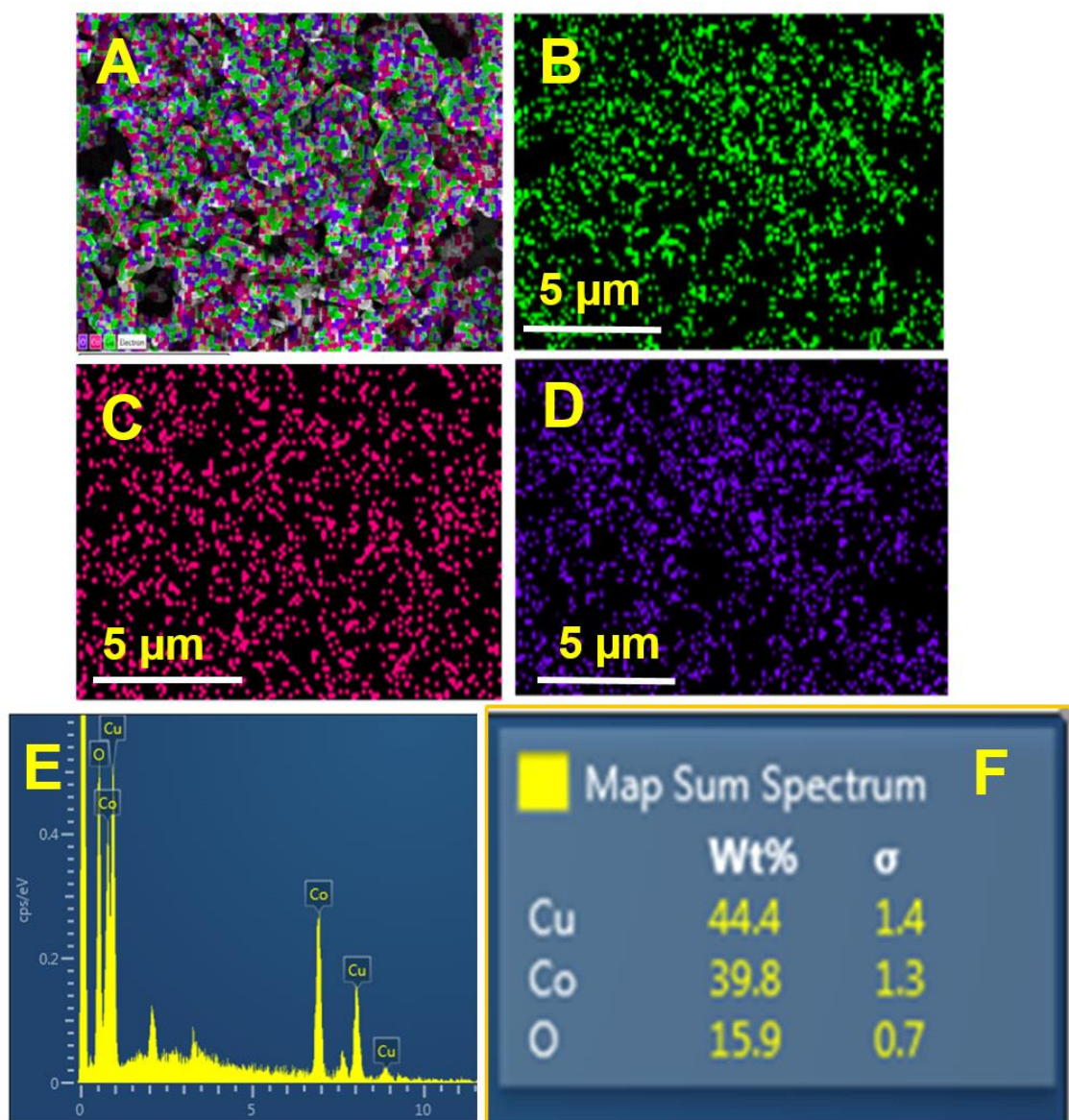


Figure 2. Elemental mapping of (A) CuCoO_2 , (B) Cu; (C) Co; (D) O; (E) EDS spectrum of CuCoO_2 , and (F) elemental ratio of CuCoO_2 .

3.2. Electro-reduction of FTD at differently modified electrodes

Figure 3A shows the electrochemical behavior of separate modified electrodes such as (a) bare SPCE, (b) activated SPCE, (c) ASPCE/CuCoO₂ electrodes in PBS (pH 7) containing 200 μM FTD at a scan rate of 50 mVs^{-1} . The CV of ASPCE/CuCoO₂ electrodes shows the absence of FTD at a scan rate of 50 mVs^{-1} . The CVs of bare SPCE displayed a peak current of 107 μA , but there is no obvious peak for FTD reduction at the potential range of (0 to -1.0 V). However, the SPCE electrode shows the reduction peaks (E_p) at -0.14 V and peak currents (I_{pc}) at 206 μA . In addition, the SPCE/CuCoO₂ electrode exhibits a sharp FTD reduction peak (E_{pc}) at -0.53 V and peak current (I_{pc}) at 369 μA (**Figure 3B**). For the ASPCE/CuCoO₂ electrode, there is no peak appearing without the addition of FTD. Undoubtedly, the ASPCE/CuCoO₂ electrode turns into the finest electrode material for the electrocatalytic reduction of FTD related to the formerly described FTD sensor.

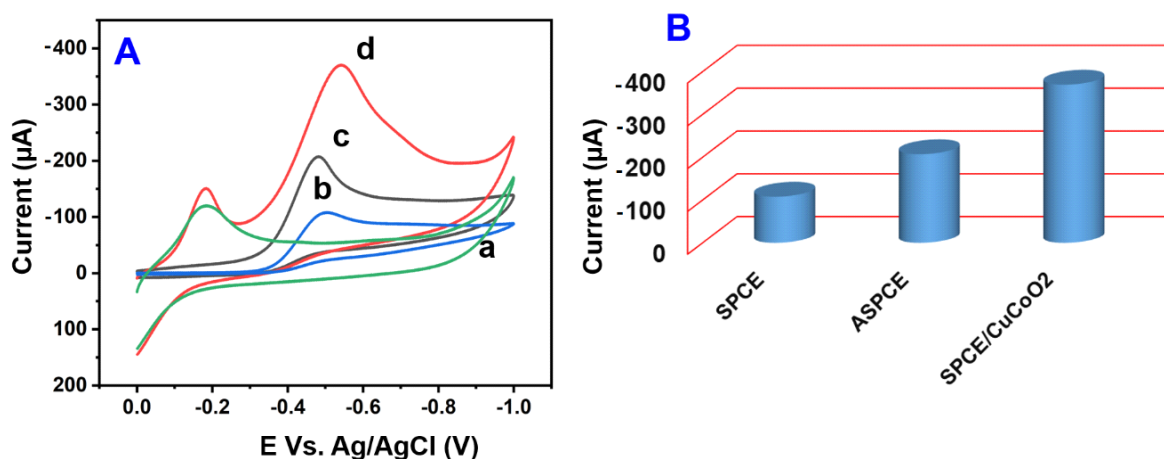


Figure 3A, CV response of (a) SPCE, (b) ASPCE, (c) ASPCE/CuCoO₂ in presence of 20 μM FTD in nitrogen-saturated PBS (pH = 7) at a scan rate 100 mV s^{-1} , (d) ASPCE/CuCoO₂ without addition of FTD. (B) Bar diagram of different film peak current.

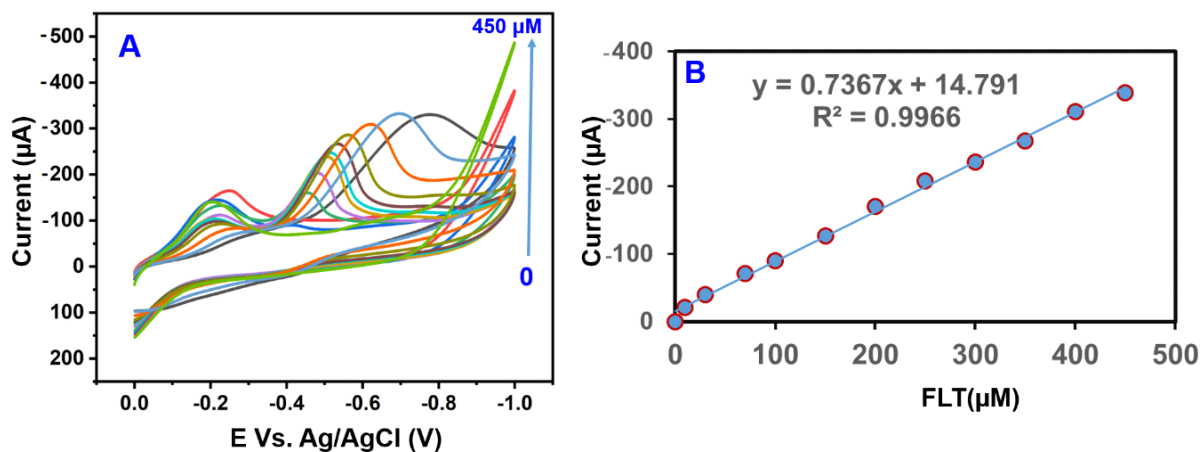


Figure 4. (A) CV response of ASPCE/CuCoO₂ at various concentrations (0-450 μM) of FTD in 0.05 M PBS (pH = 7) at 50 mVs^{-1} . (B) The linear plot between FTD (μM) Vs Peak current (I_{pc}).

The Cyclic voltammetry (CV) of ASPCE/CuCoO₂ for the different addition of FTD (0.1 μM) in the PBS with at the scan rates 50 mV s⁻¹, while increasing the concentration of FTD the cathodic peak current has increased and which shows the linear connection between the cathodic peak current and concentration of FTD representing as $I_{pc} (\mu A) = 0.7367 v + 14.791 (mVs^{-1})$ (Figure. 4A). The corresponding correlation coefficient is exhibited at 0.9966 (Figure. 4B). The following results represent that the ASPCE/CuCoO₂ shows an excellent electrode for the finding of FTD.

3.3. Effect of pH and scan rates

CV was used to study the effect of pH on the performance of as-prepared modified electrodes for FLD detection. The CV experiment was carried out at ASPCE/CuCoO₂ at pHs ranging from 1 to 9 to electro catalytically oxidize 200 μM of FTD. As demonstrated in Figure. 5A, increasing the electrolyte pH from 3 to 7 raised the reduction peak current of FTD, while altering the pH from 7 to 9 decreased. Figure. 5B shows the peak current at the ASPCE/CuCoO₂ was obtained to be higher in pH7 than that of other pH solutions. Besides, Figure. 3C shows the calibration plot between pH vs E_{pc} shows the linear relation. Therefore, pH 7 has taken for further electrochemical studies.

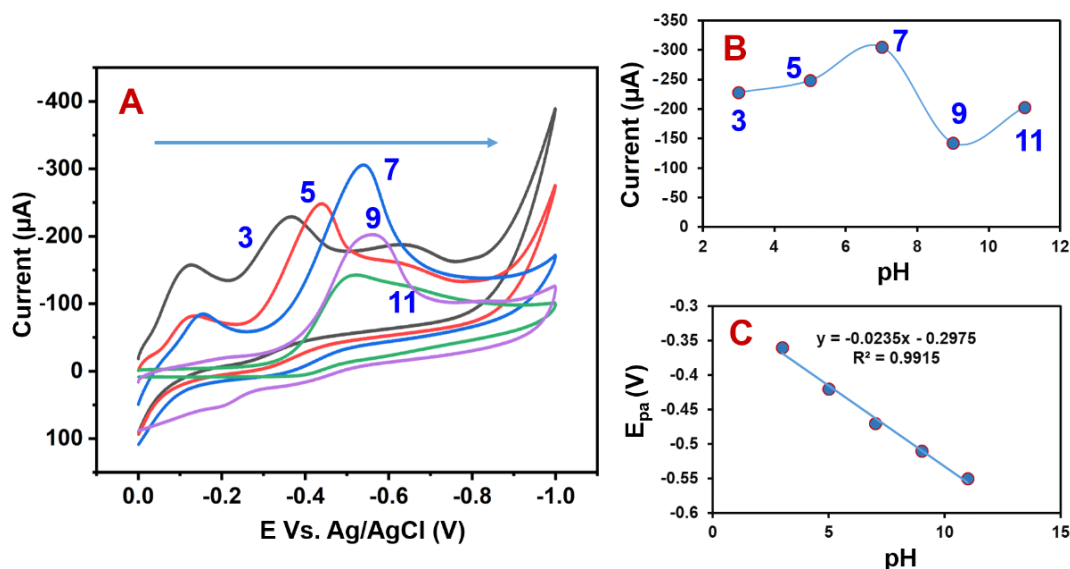


Figure 5. (A) Cyclic voltammetry response of ASPCE/CuCoO₂ modified GCE in 100 μM FTD containing different pH solutions (3, 5, 7, 9 & 11) at the scan rate of 50 mVs⁻¹, (5B) The calibration plot between pH vs I_{pc} . (5C) The calibration plot between pH vs E_{pc}

Figure. 6(A), shows a typical CV curve obtained at the ASPCE/CuCoO₂ electrode for the different scan rates containing 200 μM FTD in PBS (pH 7). The cyclic voltammograms found at ASPCE/CuCoO₂ in N₂ saturated PBS at various scan rates with the increasing of scan rates from (10-180 mVs⁻¹), the cathodic peak (I_{pc}) current of FTD was increased. Furthermore, the cathodic peak potential shifted to a positive value (10-180 mVs⁻¹). Figure. 6(B) indicated the calibration plot represents the linear relation connecting the cathodic peak current expressed as $I_{pc}(\mu A) = 1.6617v + 13.462 (mVs^{-1})$,

with an interaction coefficient of 0.9909. The result represents that the electrochemical detection of FTD at ASPCE/CuCoO₂ is an adsorption-controlled process. Those performances reveal that the ASPCE/CuCoO₂ has an excellent performance in the detection of FTD.

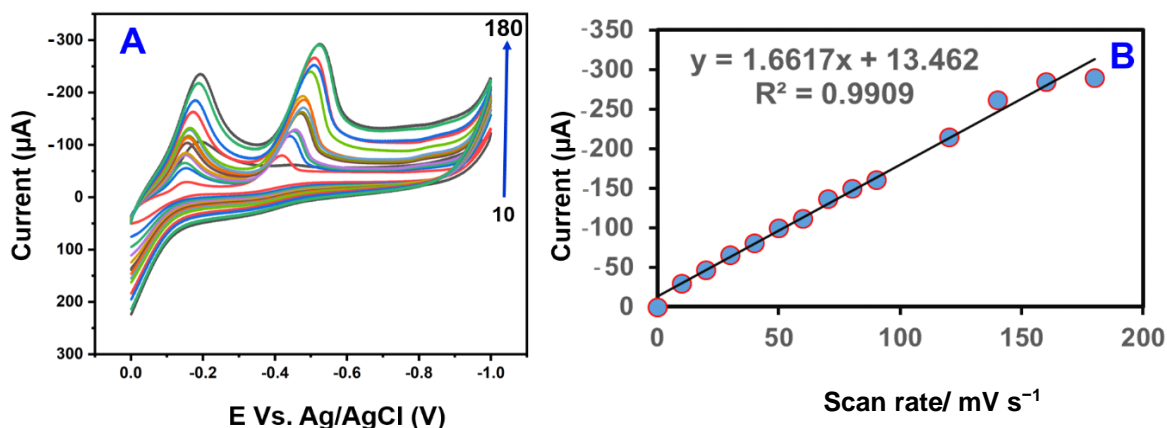


Figure. 6A, Cyclic voltammetry response of the ASPCE/CuCoO₂ electrode in PBS containing 100 µM of FTD at different scan rates (10-180 mV s⁻¹). **(6B)** Calibration plot of scan rate Vs peak current (*I_p*).

3.4. Differential pulse voltammetry studies

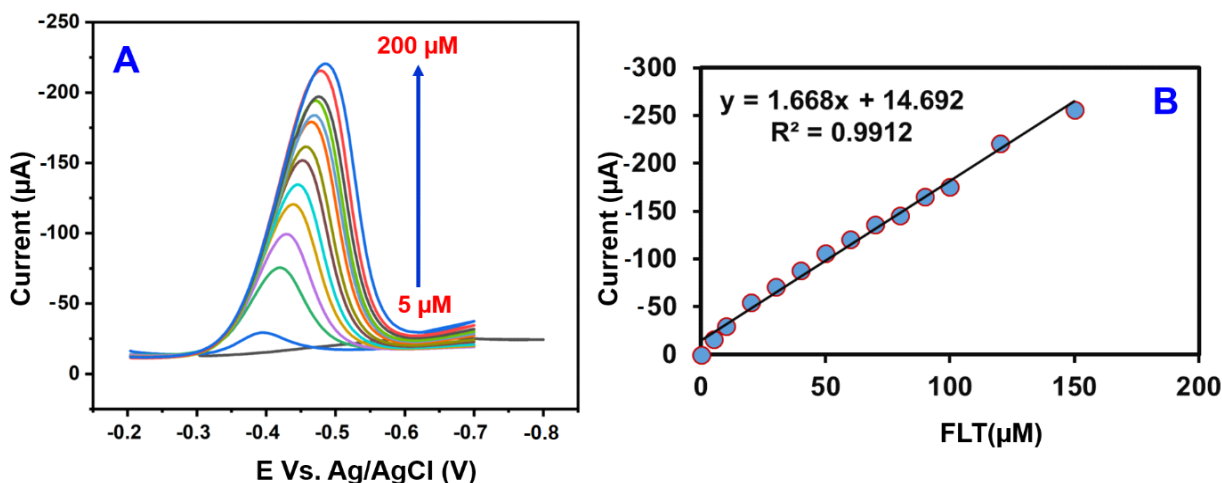
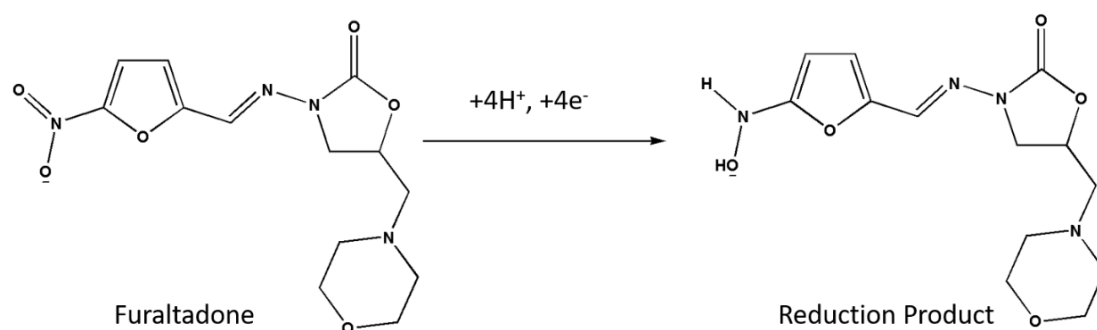


Figure 7 (A), DPV studies of the addition of different concentrations of FTD in 0.05 M PB solution. Fig 7(B) The calibration plot between peak current vs FTD concentration.

Figure. 7A represents the DPV performance of the detection of FTD by the electrochemical method on the ASPCE/CuCoO₂ electrode. The studies of DPV by ASPCE/CuCoO₂ were accomplished by the potential scanning from (-0.1 to -0.9) with an accretion time of 180 s. The DPV retort of ASPCE/CuCoO₂ represents the sharp cathodic peak were obtained for the disparate addition of FTD into +the PBS. The DPV studies represent the cathodic peak (*I_{pc}*) current increased on the successive addition of FTD. Besides, **Figure. 7B** represents the straightaway calibration of cathodic peak current (*I_{pc}*) vs FTD (M) concentration and it was disported to be $I_{pc} = 1.668 [\text{FTD}] (\text{M}) + 14.692$ with the correspondence

coefficient of $R^2=0.9912$. According to DPV experiments, the detection of FTD on the ASPCE/CuCoO₂ has an acceptable linear concentration range (0.1–220 μM), a low detection limit (3.4 nM), and a greater sensitivity (11.2598 $\mu\text{A}\mu\text{M}^{-1}\text{cm}^2$). Furthermore, the ASPCE/CuCoO₂ electrode analytical performance was compared to those of previously described FTD sensors, as shown in **Table 1**. Accordingly, the detection limit of the ASPCE/CuCoO₂ electrode was lower than that of the other electrochemical FTD sensors. The sensitivity and detection limit were also compared to those of other modified electrodes that had previously been published. For instance, ZnO-ZnCo₂O₄ NH/GCE modified electrode (LOD = 34.1 nM) [36], FeVO/p-rGO-NCs fabricated electrode (LOD=138 nM) [37], HPLC-UV detection method (LOD=10.0 $\mu\text{g kg}^{-1}$) [38], LC-MS detection technique (LOD=0.5 $\mu\text{g kg}^{-1}$) [39], and ELISA identification method (LOD=0.3 $\mu\text{g kg}^{-1}$) [40]. Because of the strong catalytic activity of hexagonal CuCoO₂ complex incorporated high surface area of ASPCE [36-40]. The above result demonstrates that the ASPCE/CuCoO₂ electrode has a good electrochemical performance in FTD detection (**Scheme 2**). The high electrocatalytic CuCoO₂ also allows for a favorable interaction and synergistic impact between the FTD and the ASPCE/CuCoO₂ electrode. As a result, the proposed ASPCE/CuCoO₂ electrode is strongly recommended for detecting FTD selectively. As a result, the ASPCE/CuCoO₂ electrode has been utilized to detect FTD from antibiotic ointments in practice.



Scheme 2. Electrocatalytic reduction of Furaltadone.

3.5. Interference analysis

The RRDE/CuCoO₂ (RRDE-Ring Rotating Disc Electrode) electrode selectivity was examined using the amperometric technique (*it*). The selectivity studies of the RRDE/CuCoO₂ are very important for the determination of FTD in environmental, and pharmaceutical samples (**Figure. 8**). The electrode operating potential was held at -0.20 V, and the rotation speed was 1500 rpm for 1400 seconds. The amperometric response was well characterized by the (a) 50 μM FLD addition to the RRDE/CuCoO₂ electrode. However, no notable peak seemed after adding 100-fold excess concentrations of interfering molecules such as (b) nitrobenzene, (c) nitro-aniline, (d) p-nitrophenol, and 300 m higher concentration additions of (e) K⁺, (f) Ca²⁺, (g) Na⁺, (h) Cu²⁺, (i) Ni²⁺, (j) Fe³⁺, (k) CO₃²⁻, (l) PO₄³⁻, (m) NO₃⁻, (n) Mg²⁺, (o) hydrazine, (p) Furazolidone, (q) Nitenpyram, (r) Nitrofurazone, and (s) Ornidazole. This represents that the peak current return of FTD metal ions in no way implies the presence of other interfering ions. Interestingly, a notable amperometric reaction was calculated for the addition of 5 μM FTD into the

similar phosphate buffer having the above interfering molecules. Those developments show that the selective detection of FTD in environmental and pharmaceutical samples is attainable at the RRDE/CuCoO₂.

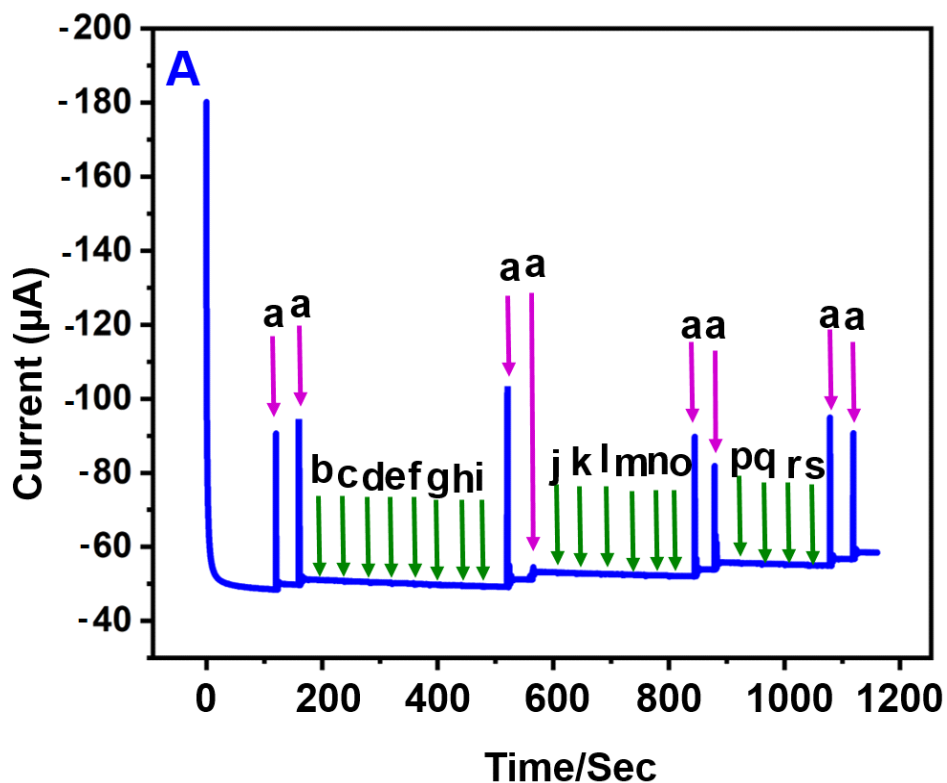


Figure 8. Amperometric response of FTD at RRDE/CuCoO₂ in the 50 µM of (a) FTD and 500 µM of interferences such as (b) nitrobenzene, (c) nitro-aniline, (d) p-nitrophenol, and 300 m higher concentration additions of (e) K⁺, (f) Ca²⁺, (g) Na⁺, (h) Cu²⁺, (i) Ni²⁺, (j) Fe³⁺, (k) CO₃²⁻, (l) PO₄³⁻, (m) NO₃⁻, (n) Mg²⁺, (o) hydrazine, (p) Furazolidone, (q) Nitenpyram, (r) Nitrofurazone, and (s) Ornidazole.

3.6 Repeatability, reproducibility, and stability studies in ASPCE/CuCoO₂

Cyclic voltammetry was used to test the ASPCE/CuCoO₂ electrode's repeatability and reproducibility in PBS containing a 20 µM addition of FLD. **Figure 9(A)** exhibited the four repeating measurements utilizing a single ASPCE/CuCoO₂ electrode, the prepared electrode had an acceptable level of repeatability, with an acceptable 2.12 percent relative standard deviation (RSD). Furthermore, **Figure 9(B)** shows the SPCE/CuCoO₂ electrode demonstrated acceptable 2.93 percent repeatability in four separate experiments utilizing four different ASPCE/CuCoO₂ electrodes. The results revealed that the modified ASPCE/CuCoO₂ electrode had good repeatability and reproducibility ability. In addition, the ASPCE/CuCoO₂ electrode operational stability was checked using a CV approach in the presence of a 20 µM addition of FLD. The FLD peak current loss was only 2.5 percent from the initial current in the experiments. The acquired results show that the system is operationally stable.

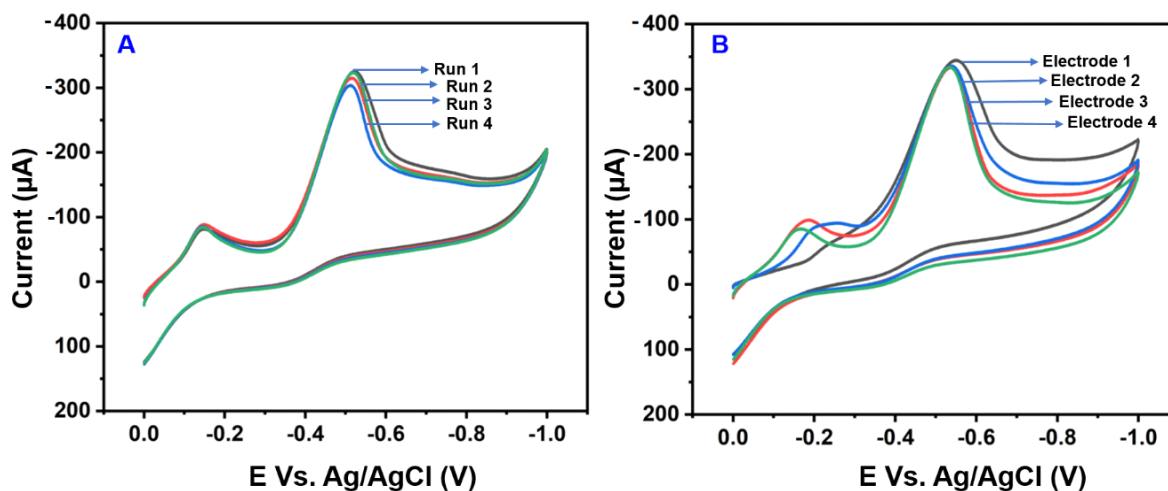


Figure 9(A) Repeatability studies of the ASPCE/CuCoO₂ modified electrode, **Figure 9(B)** Reproducibility studies of the ASPCE/CuCoO₂ modified electrode.

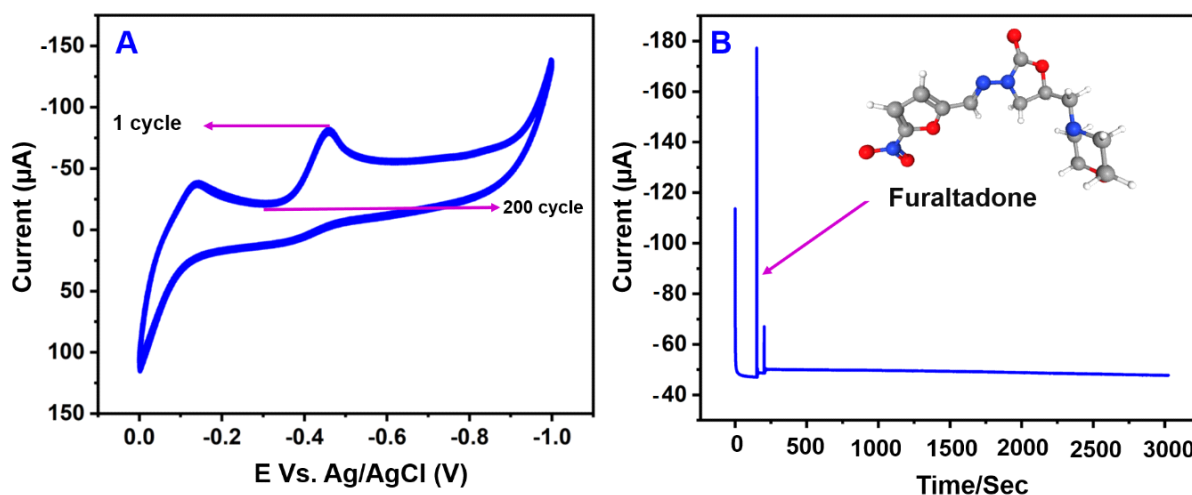


Figure 10. (A) Cyclic stability and **Figure 10(B)** functioning stability studies of the ASPCE/CuCoO₂ modified electrode.

Furthermore, the CV approach was used to examine the ASPCE/CuCoO₂ electrode cyclic stability using FLT (20 M) in conjunction with PBS (pH 7.0) and a scan rate of 50 mVs⁻¹ (**Figure. 10A**). The gained outcomes revealed the initial peak current loss from the first to the 200th cycle was less than 7%, demonstrating the superior stability of the ASPCE/CuCoO₂ electrodes in terms of FTD detection. The operational stability of the CuCoO₂/RRDE was evaluated using the amperometry method, as shown in **Figure. 10B**. The stability investigation lasted up to 3000 seconds, with the experimental conditions set at -0.4 V as a fixed potential. After a continuous run of up to 3000 seconds, the sensor retains 93.5 % of its initial current response.

3.7 Real sample analysis

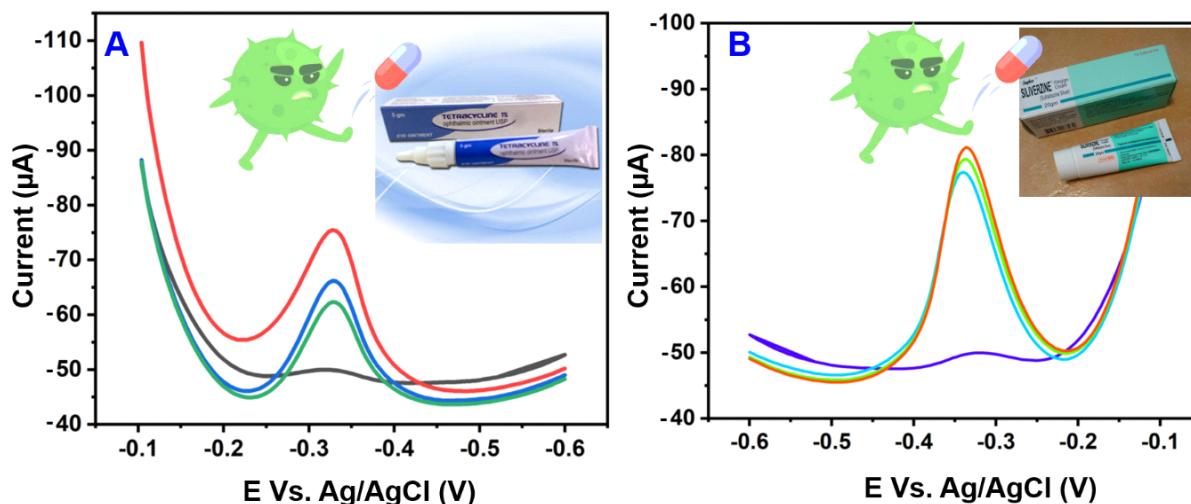


Figure 9. Real sample analysis in (A) Tetracycline and (B) Silver zinc samples using ASPCE/CuCoO₂ modified electrode.

A CV approach was used to demonstrate the practical feasibility of the CuCoO₂/SPCE sensor in Tetracycline (**Figure. 11A**) and Silver zinc (**Figure. 11B**) antibiotic ointment samples. The antibiotic ointment was purchased from a local Taiwan pharmacy shop. The collected antibiotic ointment samples were processed to make liquid samples before completing the real sample analysis. For the real sample analysis, the standard addition procedure were utilized, as shown in **Table 2** yielding recoveries of 97.3 percent and 93.5 percent, respectively. These findings demonstrated that the designed FTD sensing electrode performs well in real sample identification. As a result, the ASPCE/CuCoO₂ electrode has potential sensors in antibiotic FTD samples in pharmaceutical samples.

Table 1. Comparison of the analytical performance of ASPCE/CuCoO₂ electrode with other FTD sensors.

Investigative approach	Linear range (µM)	Limit of Detection (µM)	Reference
FeVO /p-rGO NCs	0.5 to 84	138 nM	[36]
HPLC-UV	0.05-2.0	10.0 µg kg ⁻¹	[37]
LC-MS/MSc	1–800	0.5 µg kg ⁻¹	[38]
ciELISA	0.9–105.3	0.3 µg kg ⁻¹	[39]
LC-MS/MS	0.98 to 0.99	0.2 µg/kg	[40]
ASPCE/CuCoO ₂	0.1-316	1.79 nM	This work

Table 2. Determination of FTD using different antibiotics by ASPCE/CuCoO₂ electrode.

Real samples	Added(µL)	Found(µL)	Recovery	RSD %
Antibiotic 1	10	-	-	-
	20	18	90%	-
	30	28	93%	3.9
Antibiotic 1	10	-	-	-

	20	19	91%	-
	30	29	93%	3.7

4. CONCLUSION

In brief, the CuCoO₂ complex has been successfully prepared by hydrothermal methods and applied to the selective electrochemical detection of FTD. The as-synthesized sample has been characterized by field emission scanning electron microscope, X-ray diffraction studies, and Energy-dispersive X-ray spectroscopy. The ASPCE/CuCoO₂ electrode has prosperously constructed and examined various concentrations, different scan rates, and pH by CV, DPV, and i-t studies. Therefore, ASPCE/CuCoO₂ electrode exhibited excellent electrocatalytic performance for the determination of FTD. The ASPCE/CuCoO₂ has a very good electrochemical performance with an excellent limit of detection (LOD) (1.79 nM), long linear range (1-316 μM), high sensitivity (21.03 μAμM⁻¹ cm⁻¹), selectivity, repeatability, and reproducibility. Therefore, the ASPCE/CuCoO₂ has practicable for the detection of FTD in numerous antibiotic samples with adequate reclamation. As a result, this ASPCE/CuCoO₂ electrode material is suitable for the electrochemical detection of FTD. On the other hand, in the future the prepared CuCoO₂ complex have been applied in photocatalytic and energy storage applications.

DECLARATION OF COMPETING INTEREST

The authors declare that they have no known competing financial interests or personal relationships that could have appeared to influence the work reported in this paper.

ACKNOWLEDGMENT

This work is jointly supported by the projects from NTUT-USTB-110-02, National Taipei University of Technology, and the University of Science and Technology Beijing. Financial support from the Natural Science Foundation of China (Nos. 21631003 and 22001015), Beijing Natural Science Foundation (2202028), the joint research project between the University of Science and Technology Beijing and National Taipei University of Technology (TW2019008), and Fundamental Research Funds for the Central Universities of China (No. FRF-BD-20-14A) is also gratefully acknowledged. The authors are grateful for the financial support from the Ministry of Science and Technology (MOST), Taiwan, Project no. MOST 110-2113-M-027-007 and Project no. MOST 110-2113-M-027-003. The authors appreciate the Precision Research and Analysis Centre of the National Taipei University of Technology in providing the measurement facilities.

References

1. M. Vass, K. Hruska and M. Franek, *Vet Med.*, 53 (2008) 469.
2. D. Vasu, A. K. Keyan, S. Sakthinathan, C. L. Yu, B. Z. Hsu, T. W. Chiu and J. Wu, *Electrocatalysis.*, 2022, DOI <https://doi.org/10.1007/s12678-022-00715-9>
3. E. Verdon, P. Couedor and P. Sanders, *Anal. Chim. Acta.*, 586 (2007) 336.
4. D. Vasu, A. K. Keyan, S. Sakthinathan and T. W. Chiu, *Sci. Rep.*, 12 (2022) 886.

5. Z. L. Xu, Y. D. Shen, Y. M. Sun, K. Campbell, Y. X. Tian, S. W. Zhang, H. T. Lei and Y. M. Jiang, *Talanta.*, 103 (2013) 306.
6. S. M. M. Nouri, A. R. Khadem, S. A. Hosseini and S. M. Nouri, *Environ. Sci. Pollut. Res.*, 29 (2022) 2965.
7. F. Pekdemir, I. Kocak and A. Sengul, *Electrocatalysis.*, 13 (2022) 126.
8. C. C. Wang, C. L. Yu, S. Sakthinathan, C. Y. Chen, T. W. Chiu and Y. S. Fu, *J Mater Sci: Mater Electron.*, 33 (2022) 1091.
9. K. Arjunan, R. Rajakumaran, S. Sakthinathan, S. M. Chen, T. W. Chiu and S. Vinothini, *ECS J Solid State Sci Technol.*, 10 (2021) 045011.
10. C. Y. Chen, S. Sakthinathan, C. L. Yu, C. C. Wang, T. W. Chiu and Q. Han, *Ceram. Int.*, 47 (2021) 23234.
11. S. Sakthinathan, T. Kokulnathan, S. M. Chen, R. Karthik, P. Tamizhdurai, T. W. Chiu and K. Shanthi, *J. Electrochem. Soc.*, 166 (2019) B68.
12. P. Tamizhdurai, R. Rajakumaran, S. Sakthinathan, S. M. Chen, T. W. Chiu and S. Narayanan, *Microporous Mesoporous Mater.*, 307 (2020) 110449.
13. J. V. Kumara, R. Karthik, S. M. Chen, K. H. Chen, S. Sakthinathan, V. Muthuraja and T. W. Chiu, *Chem. Eng. J.*, 346 (2018) 11.
14. J. Song, M. Huang, X. Lin, S. F. Y. Li, N. Jiang, Y. Liu, H. Guo and Y. Li, *Chem. Eng. J.*, 427 (2022) 130913.
15. S. Sakthinathan, P. Tamizhdurai, A. Ramesh, T. W. Chiu, V. L. Mangesh, S. Veerarajan and K. Shanthi, *Microporous Mesoporous Mater.*, 292 (2020) 109770.
16. G. Zhao, X. C. Wang, G. Liu and N. T. D. Thuy, *Sens. Actuators B Chem.*, 350 (2022) 130834.
17. T. T. T. Toan, D. M. Nguyen, D. M. Dung, D. T. N. Hoa, L. T. T. Nhi, N. M. Thanh, N. N. Dung, Y. Vasseghian and N. Golzadeh, *Chemosphere.*, 289 (2022) 133171.
18. F. Allahnouri, K. Farhadi, H. Eskandari and R. Molaei, *Microchimica Acta.*, 186 (2019) 676.
19. J. V. Kumar, R. Karthik, S. M. Chen, T. Kokulnathan, S. Sakthinathan, V. Muthuraj, T. W. Chiu and T. W. Chen, *Inorg. Chem. Front.*, 5 (2018) 643.
20. A. Muhammad, R. Hajian, N. A. Yusof, N. Shams, J. Abdullah, P. M. Woid and H. Garmestan, *RSC Adv.*, 8 (2018) 2714.
21. E. C. Rama and M. T. F. Abedul, *Biosensors.*, 11 (2021) 51.
22. X. Xu, P. Dong, Y. Liu and P. M. Ajayan, *J. Power Sources.*, 400 (2018) 96.
23. J. Ahmed, A. Ganguly, S. Saha, G. Gupta, P. Trinh, A. M. Mugweru, S. E. Lofland, K. V. Ramanujachary and A. K. Ganguli, *J. Phys. Chem. C.*, 115 (2011) 14526.
24. Z. Du, J. Qian, T. Zhang, C. Ji, J. Wu, H. Li and D. Xiong, *New J. Chem.*, 43 (2019) 15233.
25. Z. Du, D. Xiong, S. K. Verma, B. Liu, X. Zhao, L. Liu and H. Li, *Inorg. Chem. Front.*, 5 (2018) 183.
26. M. Isacfranklin, R. Yuvakkumar, G. Ravi, M. Pannipara, A. G. A. Sehemi and D. Velauthapillai, *Mater. Lett.*, 296 (2021) 129930.
27. Z. Du, J. Qian, J. Bai, H. Li, M. Wang, X. Zhao and D. Xiong, *Inorg. Chem.*, 59 (2020) 9889.
28. Z. Du, D. Xiong, S. K. Verma, B. Liu, X. Zhao, L. Liu and H. Li, *Inorg. Chem. Front.*, 5 (2018) 183.
29. J. Ding, L. Li, H. Zheng, Y. Zuo, X. Wang, H. Li, S. Chen, D. Zhang, X. Xu and G. Li, *ACS Appl. Mater. Interfaces.*, 11 (2019) 6042.
30. R. A. D. D. Faria, Y. Messaddeq, L. G. D. Heneine and T. Matencio, *Int J Biosen Bioelectron.*, 5(1) (2019) 1-2.
31. S. Ku, S. Palanisamy and S. M. Chen, *J. Colloid Interface Sci.*, 411 (2013) 182.
32. S. Sakthinathan, A. K. Keyan, R. Rajakumaran, S. M. Chen, T. W. Chiu, C. Dong and S. Vinothini, *Catalysts.*, 11 (2021) 301.
33. C. L. Yu, C. H. Weng, R. J. Huang, S. Sakthinathan, T. W. Chiu and C. Dong, *Ceramics.*, 4 (2021) 364.

34. H. J. Wu, Y. J. Fan, S. S. Wang, S. Sakthinathan, T. W. Chiu, S. S. Li and J. H. Park, *Nanomaterials.*, 9 (2019) 1252.
35. S. Sakthinathan, T. Kokulnathan, S. M. Chen, R. Karthik and T. W. Chiu, *Inorg. Chem. Front.*, 5 (2018) 490.
36. R. Rajakumaran, S. M. Babulal, S. M. Chen, R. Sukanya, R. Karthik, P. M. Shafi, J. J. Shim and C. Y. Shiuan, *Appl. Surf. Sci.*, 569 (2021) 151046.
37. E. Horne, A. Cadogan, M. O. Keeffe and L. A. P. H. Boom, *Analyst.*, 121 (1996) 1463.
38. J. Barbosa, A. Freitas, J. L. Mourao, M. I. N. Silveira and F. Ramos, *J. Agric. Food Chem.*, 60 (2012) 4227.
39. C. Yan, J. Teng, F. Liu, B. Yao, Z. Xu, L. Yao and W. Chen, *Microchem. J.*, 159 (2020) 105414.
40. C. Bock, P. Gowik and C. Stachel, *Biomed Life Sci.*, 856 (2007) 178.

© 2022 The Authors. Published by ESG (www.electrochemsci.org). This article is an open access article distributed under the terms and conditions of the Creative Commons Attribution license (<http://creativecommons.org/licenses/by/4.0/>).